Comparative Study of Thermal Water Pumping Cycles

Y.T. Abirham
Interdisciplinary Graduate School of Engineering Sciences, Kyushu University

K. Thu
Interdisciplinary Graduate School of Engineering Sciences, Kyushu University

Miyazaki, T.
Interdisciplinary Graduate School of Engineering Sciences, Kyushu University

Takata, N.
Interdisciplinary Graduate School of Engineering Sciences, Kyushu University

https://doi.org/10.5109/4372284

出版情報：Evergreen. 8 (1), pp.239-248, 2021-03. 九州大学グリーンテクノロジー研究教育センター
バージョン：

Comparative Study of Thermal Water Pumping Cycles

Y.T. Abirham[1*], K. Thu[1,2], T. Miyazaki[1,2] and N. Takata[1]

[1]Interdisciplinary Graduate School of Engineering Sciences, Kyushu University, 6–1 Kasuga-koen, Kasuga, Fukuoka 816–8580, Japan

[2]International Institute for Carbon-Neutral Energy Research, Kyushu University, Motooka, Nishi Ward, Fukuoka 819–0385, Japan

*Author to whom correspondence should be addressed:
E-mail: abirham.yemanebirhan.928@s.kyushu-u.ac.jp

(Received November 5, 2020; Revised March 25, 2021; accepted March 26, 2021).

Abstract: This study presents the attempt made to develop an ideal equivalent system for adiabatic expansion type thermal pumps found in the literature. The purpose of developing the ideal system is to investigate the maximum achievable performance of such systems irrespective of the system sizing and pump design adopted and obtain a characteristic efficiency. An ideal system was developed and analyzed. Then the system performance was compared with literature data, which was found to be reasonable. The comparison of the ideal performance of such systems with existing cycles revealed that the efficiency of such types of pumping systems is limited.

Keywords: solar-thermal; thermodynamic cycle; unconventional pumps; water pumping

1. Introduction and background

The increasing global energy demand, the emissions from the use of scarce primary energy sources, and the associated impact on the environment have brought a challenge to our society. The scientific community has been responding to this challenge from multiple directions, such as; the improvement in the efficiency of energy systems, recovery of wasted heat, investigation of environmentally benign alternative chemicals[1)] and systems[2–4)], among others. Despite the numerous efforts to combat the environmental impacts, the climatical effects have long been experienced in many aspects of our life, among which agriculture is one.

Nowadays, powered irrigational systems are widely being used for agricultural fields to increase the field output and decrease the dependency on rainfall[5,6)], which has become rather inconsistent with the recent climatic changes[7)]. Powered irrigation systems have been realized through the use of diesel or solar Photovoltaic (PV) powered water pumping systems, with the later one gaining more acceptance[8)].

However, the adoption of these technologies to the wide agricultural fields of developing countries, such as in the Sub-Saharan Africa, seems to be slow[9)]. One of the reasons for the slow adoption of these systems is due to the high initial costs and the limited availability of electricity, technical assistance, and supplies to these remote areas.

Due to these factors, many researchers in the past have put their effort towards developing another class of water pumping systems, so-called solar-thermal pumps[10–12)]. The thermal to hydraulic energy conversion in these systems can be achieved with conventional thermodynamic cycles coupled with conventional pumps. However, the adoption of specially designed pump configuration could be promising for lower system cost, local manufacturability, and maintenance, which approaches the UNDP's scheme of Village Level Operation and Maintenance (VLOM) initiative in addition to the environmental friendliness. Hence, in the literature, various designs of pumps were proposed with different operating principles, so-called *unconventional pumps*. Some of the proposed systems outline specially designed units[13)] while others feature diaphragm membranes[14,15)], interconnected system of tanks[16,17)], liquid pistons[18)], and solid piston[19)] to transmit the pressure developed using a heat source to the liquid being pumped.

Despite the high variability of design and operation of the proposed systems, the underlying fundamental principle stays the same. The high-pressure developed during the evaporation of a liquid upon heating is used to push water to a higher elevation, and the partial vacuum created on subsequent condensation is used to lift water from the source at a lower elevation. Usually, the solar energy collected in a solar thermal collector serves as the heat source (boiler), while the delivery water serves as the sink.

One of the earliest works on such types of systems was proposed by D.P. Rao et al.[20)] in 1976. A low boiling point

working fluid (n-pentane) was heated in a flat plate solar collector. The developed pressure was directly used to create an isobaric expansion in a cylinder, displacing the water contained in it. Despite the drawback of direct contact of working fluid with the delivery water and premature condensation, the work is pioneering. K. Sudhakar et al.[21] proposed a similar family of pump with isobaric expansion but with two working fluids. Air was introduced as a secondary working fluid in order to avoid direct contact between delivery water and the primary working fluid (n-pentane). A. Venkatesh et al.[22] reported marginal improvements in performance by the introduction of a separate vapor storage tank between the solar collector and expansion cylinder. This has resulted in the change of the expansion process from isobaric to adiabatic one. The thermodynamic analysis of the typical system was also presented in the study. K. Sumathy[16] studied the behavior of a similar adiabatic expansion thermal pump for different delivery heads. In 2017, R. Bandaru et al.[23] presented the performance prediction of an isentropic expansion type solar thermal water pump for different working conditions by using an artificial neural network model. The system has similarities to that of K. Sumathy and Y.W. Wong's system[24]. A. Date et al.[25] presented a new thermodynamic ideal cycle for thermal pumping, called the Thermal Power Pump (TPP) cycle, which consists of two isochoric and two isobaric processes. It was proposed to have the potential for higher theoretical performance. N. Kurhe et al.[26] studied a solar thermal pump using a diaphragm arrangement. Even though the details of the thermodynamic cycle were not provided, it can be anticipated to be an isobaric expansion cycle, based on the outlined operation of the system.

Generally, the research works discussed above may be put into two major categories, depending on the manner of work extraction process: isobaric and adiabatic expansion. For the isobaric expansion type of thermal pumps[19–21,26], the ideal TPP cycle can be used as the maximum limit to analyze their performance. However, for the thermal pumps with adiabatic expansion[16,23,24,27–29], the presented thermodynamic cycles are dependent on the system design. Additionally, the primary working fluid used in the systems is distributed into different subsystems, which would be separated during the operation of the pump. This brings difficulty towards the analysis of an ideal thermodynamic system that would represent such a system. Due to this, a corresponding ideal cycle that serves as an ideal reference irrespective of the design variations for such type of adiabatic expansion thermal pumps is lacking, and the information available regarding the systems' ideal performances is limited. If such an ideal cycle exists, the maximum achievable performance and the room available for improvement of such family of pumps can be analyzed and compared with existing cycles.

Therefore, the goal of the present study is to analyze an equivalent ideal system for the adiabatic expansion thermal pumping systems with flexibility in system design and to investigate opportunities for improvement through a comparative study with existing cycles.

2. Theoretical Analysis

2.1 Equivalent ideal system

The performances of the adiabatic expansion thermal pumps discussed earlier are made up of series of interconnected containers of a certain size coupled with a solar collector. The performance of the system is affected by the sizing of these components since it affects the delivery head and volume pumped per cycle. By assuming an equivalent ideal system, these parameters can be varied, which allows the evaluation of the ideal scenario of the system. For this purpose, few changes are made to the existing systems to make an ideal cycle while maintaining the basic functionality and operation. The resulting equivalent ideal cycle is presented in Fig.1.

In the real systems, such as that of K. Sumathy[16], the primary working fluid (low boiling point organic fluid, such as n-pentane) is heated inside a solar collector, which evaporates it. The vapor develops pressure, and it will move through a liquid-vapor separation tank and accumulate in a vapor storage tank before the beginning of the pumping stroke. In the idealized system presented here, the solar collector, separation tank, and vapor tank of the existing systems are combined and represented by an ideal frictionless, piston-cylinder device (labeled 'VT' in Fig.1). Similarly, the condenser is represented by the second piston-cylinder device (labeled 'C' in Fig.1). ('VT' and 'C' stand for the vapor tank and condenser, respectively)

Initially, a small amount of primary working fluid is fed into VT (Fig.1a). The amount of the primary working fluid is controlled so that it will be enough to do the necessary delivery work upon expansion. When heat is applied to the liquid working fluid in a reversible manner, the temperature and pressure increase, pushing the piston-1 upwards, with external weight placed on it. The applied weight is used to constrain the pressure in VT to a preset value. The pressure inside this cylinder corresponds to the initial pressure of vapor before expansion (pumping) starts. Hence, depending on the required delivery head, this initial pressure can be varied by controlling the weight on the piston.

As the heat addition continues, the working fluid in VT is completely vaporized, and the piston reaches the top dead center (TDC) of the cylinder (Fig.1b). Then, the heat source and the weight on the piston are removed and replaced by insulation; the piston position is fixed at the TDC, and Valve 1 (V1) is opened. These sets of operations allow the vapor to expand adiabatically into the water tank (WT), as shown in Fig. 1b. As a result, the water in WT is transferred to the air tank (AT), which simultaneously compresses the air until it reaches the delivery pressure. At this state, the compressed air starts to displace the water in the delivery tank (DT), resulting

to the pumping of water from DT to a higher elevation. When the water level in WT reaches the minimum position, the delivery process is completed; hence, valve 2 (V2) is opened, allowing the vapor to further expand to atmospheric pressure in C (Fig.1c). Then C is put in

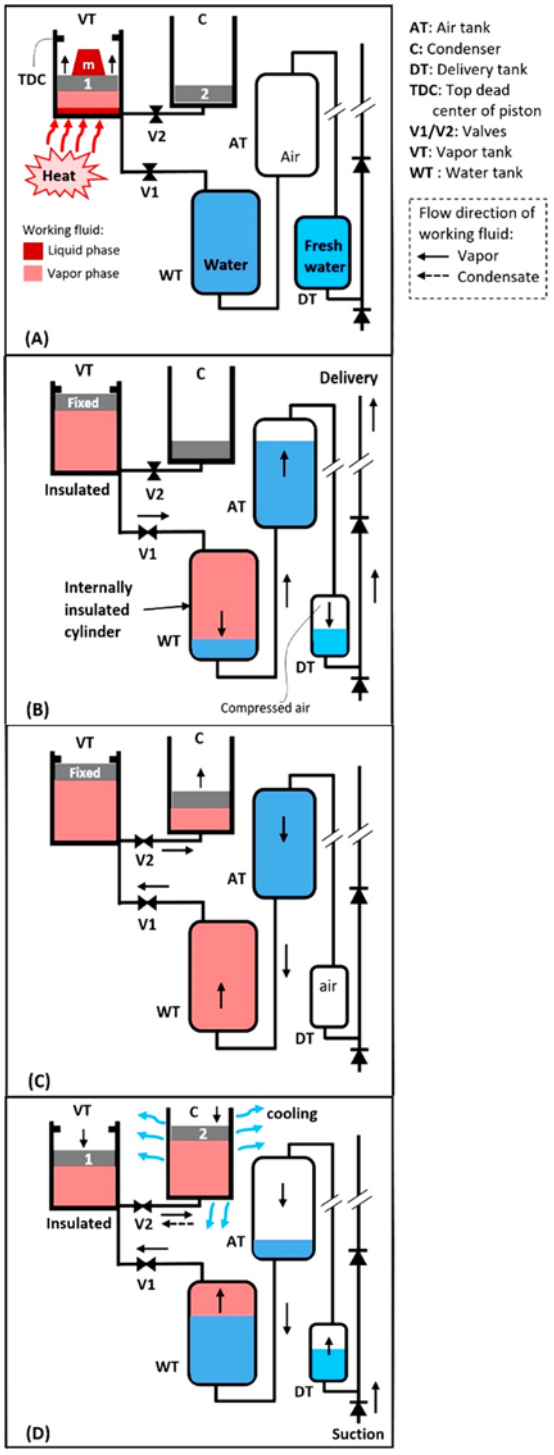

Fig. 1: An idealized system representation of a thermal pump

contact with a heat sink, which causes the condensation of the vapor in the cylinder. Simultaneously, the compressed air in the delivery tank (DT) starts to expand, pushing the water from AT back to WT, (the volumes of AT and WT are kept same in this study). The subsequent decrease in the pressure of DT allows water to enter it under atmospheric pressure. However, it should be noted that significant partial vacuum is not created in this type of system to actuate suction stroke; instead, the delivery tank is immersed in a well of the water source. The pumping action/pressure pulse is transmitted by the secondary working fluid (Air). Hence, for this ideal system, the suction pressure is assumed to be atmospheric.

As the heat rejection from the condenser continues, the pressure in both VT and C falls, causing the pistons to retract to their initial position. The condensate returns into VT, completing the cycle. For this ideal cycle, the condensation of the primary working fluid is assumed to take place in the C only.

For the real systems, energy is expended in transporting the vapor produced in the solar collectors to the vapor storage tank before expansion; hence it is not directly applied in the process. Therefore, in the ideal system here, it is represented by the work done in pushing the piston in VT upwards up to the TDC, at the maximum initial pressure required for the delivery stroke of the pump. The piston's mass is to be set to match the required minimum pressure of the cycle, depending on the delivery pressure considered. Similarly, the volumes of component tanks can also be changed to explore various simulation scenarios.

2.2 Thermodynamic analysis

The schematic outline of the analysis of this system is presented in Fig. 2. The analysis starts with preset values of the delivery head and volume. The respective delivery pressure is calculated by Eq. (1), while the delivery volume is kept constant at 1 liter for all the analysis scenarios.

$$P_d = \rho g H_d + P_{atm} \quad (1)$$

where: ρ, g, H_d, and P_{atm} denote the density of water, gravitational acceleration, delivery head, and atmospheric pressure, respectively. Based on the above input values and considering air as an ideal gas, the amount of air required per cycle is estimated by assuming isothermal compression. The air contained in AT is compressed from atmospheric to delivery pressure level before the pumping stroke starts in each cycle. This compression process is assumed as an isothermal process through the assumption of ideal heat exchange between air tank, air pipes, and the environment. The required air tank size, amount of air, and the respective isothermal compression work done are estimated by the following three equations, respectively.

$$V_a = \frac{P_d V_d}{P_{atm}} \quad (2)$$

$$m_a = \frac{P_{atm} V_a}{R T_0} \quad (3)$$

$$W_a = m_a R T_0 \ln \frac{V_d}{V_a} \quad (4)$$

where: V_d, R and T_0 represent the delivery water volume per cycle, the ideal gas constant of air, and the ambient temperature.

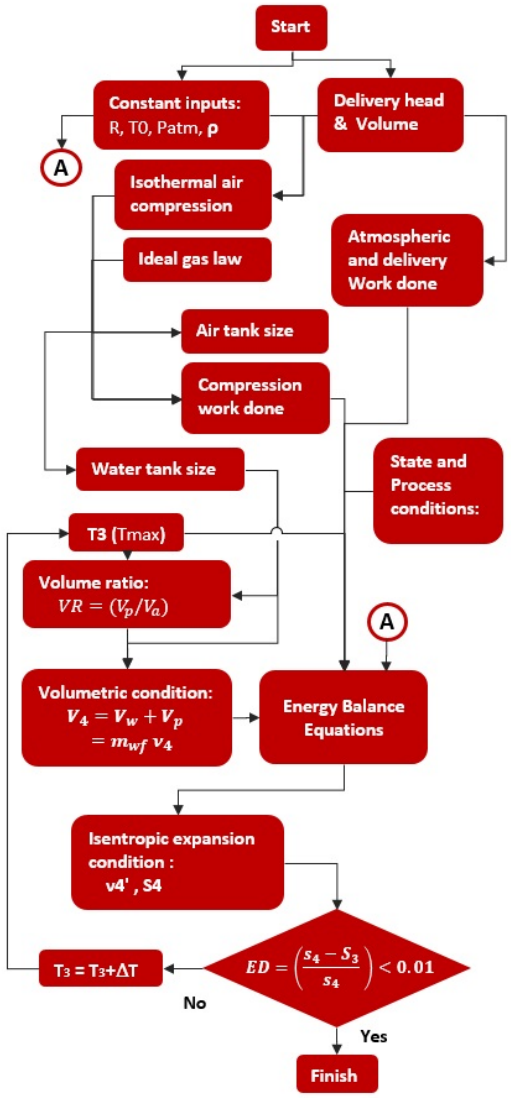

Fig. 2: Schematic outline of the analysis procedure

The delivery work done on the water and the atmosphere are calculated as follows, respectively.

$$W_d = V_d \rho g H_d \quad (5)$$

$$W_{atm} = V_d P_{atm} \quad (6)$$

Hence, the total work output required from the cycle is given by the following equation.

$$W_{out} = W_d + W_{atm} + |W_a| \quad (7)$$

The small quantity of working fluid that is initially fed into the VT is assumed as the thermodynamic system, and it is assumed to undergo the following ideal processes to constitute the necessary equivalent ideal cycle for the adiabatic expansion thermal pumps.

- Process 1-2: Isochoric heating
- Process 2-3: Isobaric sensible and latent heat addition
- Process 3-4: Isentropic expansion (pumping)
- Process 4-5: Isentropic expansion (to the condenser)
- Process 5-1: Isobaric cooling

The corresponding system states are:
State 1: Saturated liquid, **State 2**: Compressed liquid, **State 3**: Saturated vapor at a maximum pressure of the cycle
State 4: A state corresponding to the entropy at state-3 and at the delivery pressure. **State 5**: A state corresponding to the entropy at state-3 and atmospheric pressure.

The cycle formed by these processes will partially resemble the TPP cycle and Organic Rankine Cycle (ORC); however, the total useful work output from the cycle will be limited since the expansion work (pumping) cannot be done beyond the delivery pressure.

The energy balance of the individual processes is carried out using the following equation.

$$\Delta U = Q + W \quad (8)$$

The net-work output from the cycle is given by the following equation.

$$W_{net} = W_{23} + W_{34} + W_{45} + W_{51} \quad (9)$$

$$W_{23} = P_3 m_{wf} (v_2 - v_3) \quad (10)$$

$$W_{45} = m_{wf} (u_5 - u_4) \quad (11)$$

$$W_{51} = P_{atm} m_{wf} (v_5 - v_1) \quad (12)$$

where: m_{wf} denotes the mass of the working fluid whereas; u represents the internal energy of the system at the respective states. The terms W_{23} and W_{34} denote the work output during the isobaric and isentropic expansion processes, respectively, whereas W_{51} indicates the work input to the cycle. As discussed earlier, the isobaric expansion work, W_{23}, is not available for pumping for this type of thermal pump, as it represents the expansion of vapor from a solar collector to a vapor storage tank in real systems. The term, W_{45}, represents the expansion of the primary working fluid to the condenser chamber at the end of pumping stroke. Therefore, the useful work output from the cycle is limited, as shown in the following equation.

$$W_{out} = W_{34} = m_{wf}(u_3 - u_4) \quad (13)$$

The total heat input and system efficiency are given by the following equations, respectively.

$$Q_{in} = Q_{12} + Q_{23} = m_{wf}(h_3 - h_1) \quad (14)$$

$$\eta = \frac{W_d}{Q_{in}} \quad (15)$$

where: Q_{12} and Q_{23} are the heat inputs for the respective processes, and h denotes the enthalpy of the system.

In addition to the energy balance equations, the analysis will be constrained by the volumetric requirement that the system needs to meet in order to achieve the preset delivery volume and head. That means, in addition to the amount of vapor required to perform the necessary pumping work, there will be an additional quantity of vapor required to displace and compress the air in AT. Hence, at the end of the delivery process, state-4, the vaporized working fluid, needs to occupy both the vapor and water tanks at the delivery pressure, *Eq. (16).*

$$V_4 = m_{wf}\mathrm{v}_4 = V_w + V_p \quad (16)$$

$$V_\mathrm{p} = V_3 = m_{wf}\mathrm{v}_3 \quad (17)$$

where V and v are the volume of the system and specific volume at the respective states. V_w and V_p are the sizes of the water and vapor tanks, respectively.

At state-3, the working fluid vapor fully occupies the VT, and its amount should be enough to extract the required amount of work (W_{out}). Hence, the vapor tank volume is specified based on the pressure and vapor density at state-3, Eq. (17). The minimum pressure required in the vapor tank before the pumping process for a specific amount of work output is not known, hence the procedure outlined in Fig. 2 was followed. The temperature at state-3 (the maximum temperature of the cycle) was iterated, and the deviation of the entropy between states 3 and 4 was checked to approach the solution with isentropic expansion condition, as shown in the equation below.

$$ED = \frac{(s_4 - s_3)}{s_4} \quad (18)$$

where: s and ED denote the entropy and the difference in entropy, respectively, for states 3 & 4.

In the relevant literature, the general working fluid selection criteria discussed for thermally driven pumping systems includes non-toxicity, favorable thermophysical properties (such as low latent heat of vaporization, high thermal conductivity, and specific heat capacity), chemical stability, normal boiling point above ambient temperature, and environmental friendliness, among others. N-pentane satisfies many of these properties, and hence it was considered as the primary working fluid in the current study as well. Depending on application conditions, such as temperature and pressure limits, alternative organic working fluids can also be investigated.

3. Results and Discussion

3.1 Idealized system performance (TP-1)

The above analysis was carried out using Engineering Equation Solver[30] for the delivery head range of 1 to 20m while keeping the delivery volume constant at 1 liter per stroke. The heat source temperature was varied depending on the delivery head, and the optimum value was selected iteratively to approximate the isentropic expansion condition between states 3 & 4. The heat sink temperature was kept at the normal boiling point of the primary working fluid (n-pentane, 35.87 °C). Hence, the suction head is essentially zero, which is the case for this type of pump.

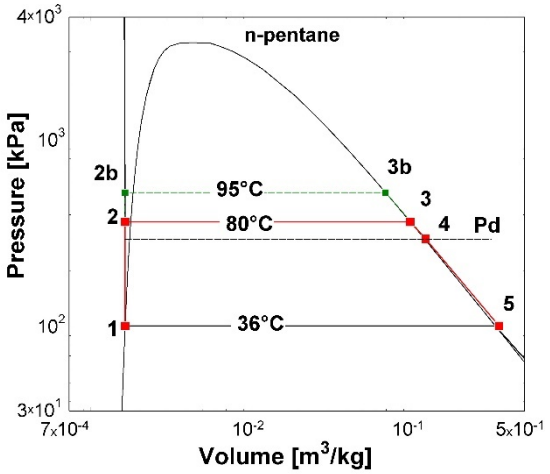

Fig. 3: Thermodynamic cycle of the idealized system

The thermodynamic cycle of the system is depicted in Fig. 3. The process paths 1-2-3-4-5-1 constitute the cycle for the corresponding heat source and sink temperatures of 80 and 36°C, respectively. Likewise, the path 1-2b-3b-4-5-1 represents the cycle for a heat source temperature of 95°C for the same delivery head.

During the solving process, the peak temperature of the cycle was initially set at a high value and iterated towards low temperature, following the schematic outlined in Fig. 2. At the early iterations of the solution, the cycle efficiencies were observed to be high. However, since the difference in entropy, *ED*, and the volumetric constraints were not satisfied, the solution iteration was continued until the *ED* value falls below 1%. In this way, the cycle efficiency of the system was calculated and recorded for each delivery heads, and the resulting characteristic curve is depicted in Fig. 4.

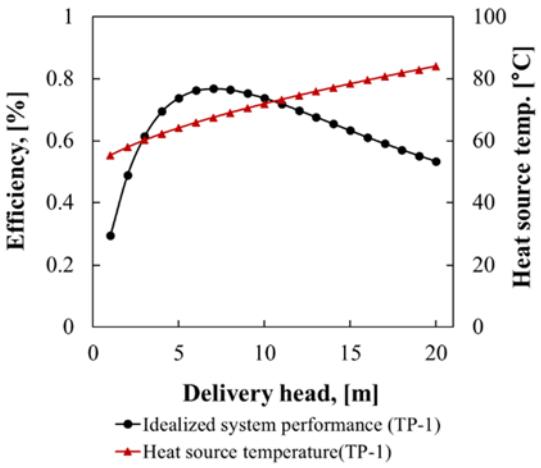

Fig. 4: Characteristic efficiency curve of the idealized cycle and the heat source temperature for various delivery heads.

The results depicted in Fig. 4 present the efficiency of the idealized system with the maximum cycle temperature (heat source temperature) required to develop the range of delivery heads under ideal conditions. The increasing and decreasing pattern exhibited by the efficiency curve seems to be the result of two influencing factors. The first is the heat source temperature and the second is the compression work requirements of the secondary working fluid (air). For the lower delivery head conditions, the increase in heat source temperature of the cycle seems to favor higher cycle efficiencies. However, for higher delivery head conditions, even though the cycle operates with higher temperature, the compression work requirements of the air, Eqn. 4, increase significantly, deteriorating the cycle efficiency. Fig. 5 shows the relative proportion of the work output from the cycle that is used for the useful pumping work (hydraulic work) and the work done on the secondary working fluid (air) to compress it to the delivery pressure level before pumping is started, every cycle. It can be seen that a significant amount of the work output from process 3-4 of the cycle isn't available for hydraulic work causing lower system performance, especially for higher delivery heads.

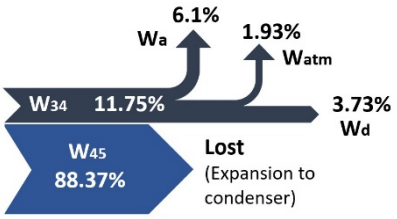

Fig. 5: Division of the work output of the pumping stroke of the cycle (process 3-4) for delivery head of 20m.

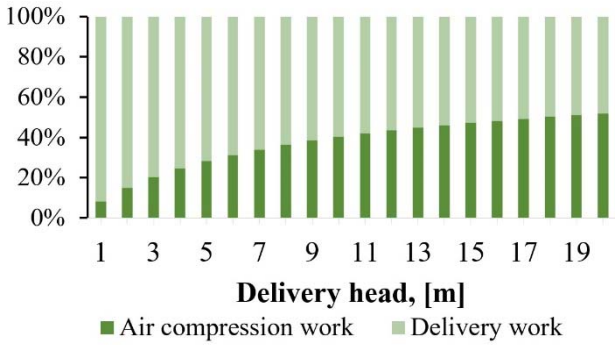

Fig. 6: The distribution of net-work output of the cycle for delivery head of 20m.

From Fig. 6, it can be observed that only the small fraction, 3.73%, of the net-work output of the ideal cycle is converted into the necessary hydraulic work. A major portion of the work potential is lost when the vapor is directed into the condenser.

An additional observation from the discussion so far is the higher amount of working fluid vapor that will be necessitated to fill the equivalent volume (*Vw*) that was initially occupied by the uncompressed air (*Va*). Even though a limited amount of working fluid would be enough to provide the work necessary for a specific delivery head and volume, there will be additional vapor requirement. Furthermore, for higher delivery heads, the necessary volume of the vapor tank (vapor volume at state 3) keeps growing in size, more than the air volume, as shown in Fig 7. As a result, the vapor requirement per cycle would be high due to the growing size of both vapor and air volumes and the associated increased compression work requirement. Hence, for higher delivery heads, even higher losses are to be expected.

The above observations encourage the investigation of a variant of the proposed ideal system with the assumption of an incompressible secondary working fluid. The variant system (TP-1B) will have a similar analysis to the idealized system discussed earlier, except to the exclusion of the air compression terms of the analysis. The result of analysis for such system, after modification, is discussed in Section 3.2 along with other cycles.

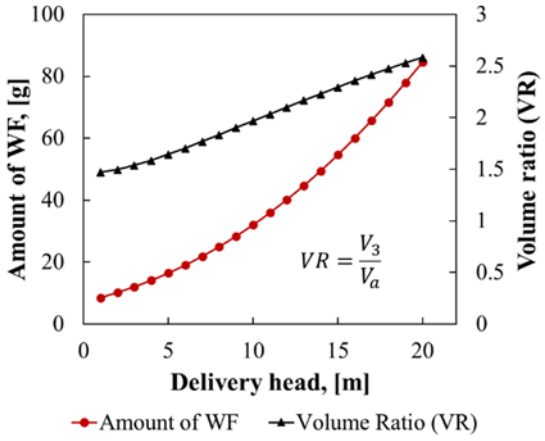

Fig. 7: Amount of working fluid required per cycle and the volume ratio of vapor and air tanks for variable delivery heads.

The obtained efficiency values of the TP-1 system are low despite the consideration of ideal system conditions. However, the results are in the same order of magnitude as the thermal pumping system performances from the literature. The typical data for such types of systems, using n-pentane as a primary working fluid is presented in Fig. 8 and Table 1 with the ideal cycle discussed here. It is to be noted that the physical system sizes studied in the data are fixed, while in the current system, it is kept flexible for the purpose of approximating the ideal scenario.

Table 1. Performance data from the literature for thermal pump type-1 with n-pentane as a primary working fluid

#	Author/(type of study)	H_d [m]	η [%]
A	A. Venkatesh et al.[22) (Experimental)	8	0.12
B	K. Sumathy[16)	6	0.14
C	(Experimental)	10	0.12
D	Y.W. Wong et al.[28)	6	0.36
E	(Theoretical)	8	0.34

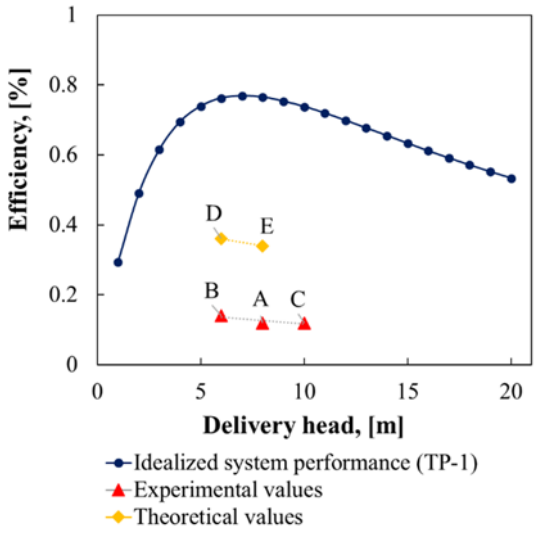

Fig. 8: Comparison of simulation result for the idealized system with data from the literature with n-pentane as a primary working fluid

The differences between the literature data and the presented ideal efficiency values are explained as follows. The system performance predicted by Y.W. Wong et al.[28)] is based on a model that accounts for realistic aspects of an experimental unit. In addition to the thermodynamic cycle analysis, the heat transfer model of the solar thermal collector was considered, and the available solar insolation has been accounted in their study. Additionally, the condition of no-pumping (preheating) was considered in their work, as the quantity of working fluid charged to the system is high. The consideration of these system dependent practical limitations will cause further reduction of the system performance. A. Venkatesh et al.[22)] discussed the presence of irriversibilities in the operation of the experimental unit such as premature condensation of vapor in the water tank, which limited the performance of the experimental unit.

The above-mentioned reasons may explain the difference observed between the literature data and the idealized system efficiency.

The results indicate that the performance of these type of thermal pumps is still limited despite ideal devices and operating conditions. Nonetheless, the simulation results can be used to compare the TP-1 type systems with existing cycles, as discussed in the following section.

3.2 Comparison of ideal cycles

The use of the idealized system of adiabatic expansion type thermal pumps makes it possible to explore the comparison of the ideal performance with existing cycles. Hence, a comparison of the ideal efficiency is carried out with two existing thermodynamic cycles, the Thermal Power Pump cycle (TPP) and Organic Rankine Cycle (ORC).

The TPP cycle is comprised of two isobaric and two isochoric processes. The cycle is intended for converting low grade heat driven pumping applications. Unlike the TP-1 system, the TPP based systems do not need the use of compressible secondary working fluid. Additionally, the delivery work is extracted during the isobaric expansion of the working fluid rather than the expansion of vapor from a higher-pressure state. Furthermore, for a similar heat sink and delivery head, the TPP cycle requires a lower heat source temperature.

The ideal cycles of TP-1 and TPP are illustrated together in Fig. 9. The process path 1-2-3-4-5-1 is for the cycle of TP-1, while path 1-2a-4-5a-1 represents the TPP cycle.

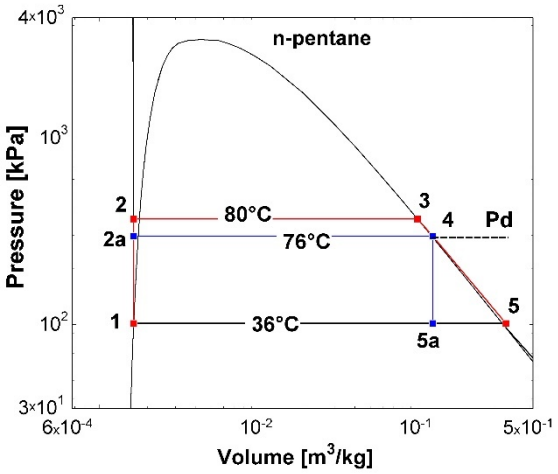

Fig. 9: Comparison of ideal cycles for TP-1 and TPP

As explained earlier, even though the working fluid in the TP-1 cycle expands to the condensation pressure after the pumping stroke, the useful works is extracted during the process 3-4 only, as the delivery pressure is fixed.

The comparison of the cycle efficiencies of the idealized cycle (TP-1) and TPP cycles is presented in Fig. 10, along with the quantity of working fluid required by the systems for the range of the delivery heads and a fixed delivery volume of 1 liter per stroke.

The difference in the performance of the two cycles, in Fig. 10, could be attributed to the high energy demand of the TP-1 system due to the increased volumetric requirement of working fluid vapor and the energy expended for the compression of air in each cycle. This can be observed in the high working fluid demand of the TP-1 cycle in the figure 10. Hence, the associated heat demand of the TP-1 is higher as the working fluid is assumed to undergo complete evaporation for both cycles.

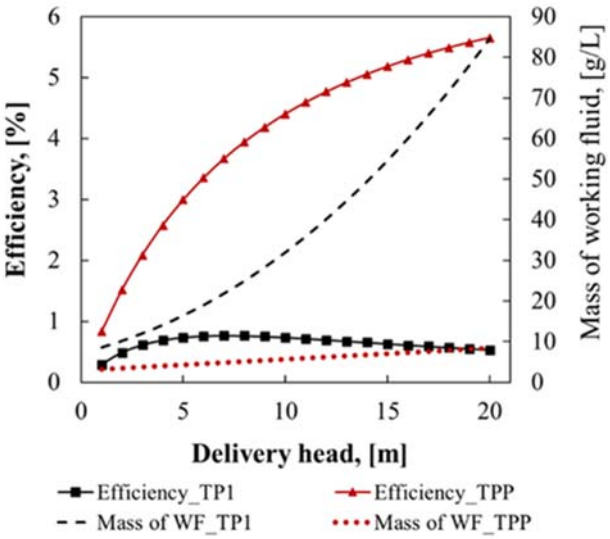

Fig. 10: Performance curves of the TP-1 and TPP cycles

The above results are compared with the corresponding thermal efficiency of a basic ORC system, operated between similar thermal limits, and working fluid, as shown in Fig. 11. The ORC would serve as a reference due to its similarity with the cycle presented here, even though it will need additional units to convert the extracted work into hydraulic work. Additionally, the scenario (TP-1B) when the TP-1 system has incompressible secondary working fluid is considered in the comparison.

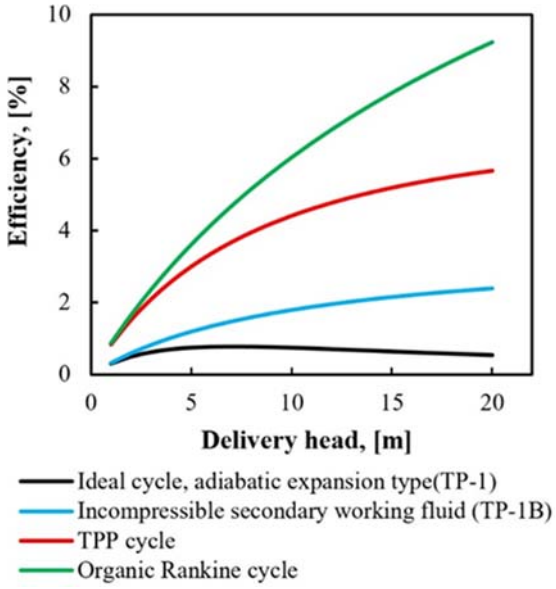

Fig. 11: Comparison of ideal cycle performance

The ORC has the highest performance, followed by the TPP, Fig. 11. The high performance of the ORC in comparison to the cycles presented, is mainly attributed to the fact that the ORC expanders have the capability to

extract useful work by expanding the pressurized vapor until it reaches near to the condensation pressure. However, for the thermal pump cycles, the pressure of the vapor cannot be further expanded beyond the delivery pressure level. As a result, their performance is lower. On the other hand, The effect of using air as a secondary working fluid is observed by comparing the efficiencies of TP-1 and TP-1B.

Based on the above observations, the adiabatic expansion type pumps seem to have limited efficiency and hence limited room for improvement in comparison to the isobaric type of systems, as shown by the TPP performance curve. However, it is to be noted that for TPP cycle-based systems, the working fluid would be different or separated from the heat transfer fluid. Hence, in real systems, the additional temperature difference would be necessary to transfer heat.

4. Conclusion

In this study, an attempt was made to develop an equivalent ideal cycle for adiabatic expansion type thermal pumping systems from the literature, and it was compared with existing cycles. The performances predicted using the ideal cycle for a range of delivery heads seem to agree reasonably with the data from the literature. Hence, the ideal system presented here may be used as a reference for a similar family of thermal pumps.

The comparison of the ideal cycle with TPP and ORC cycles showed that the current cycle has significantly lower performance. The major bottleneck for the performance of the cycle is identified to be the use of compressible secondary working fluid, which consumes a significant portion of the output work, reducing the cycle performance.

Based on the observation in this study, it is recommended to change the design of the pump so that air will not be used as a working fluid. The first suggestion would be developing a pumping system based on the TPP cycle. Secondly, it may also be possible to change the design of the pump by replacing the air with incompressible liquid to transmit the pressure developed by the system to the delivery water and placing the pumping system close to the source of the pumped liquid (water) so that the suction head requirement will be low.

Acknowledgments

The author wishes to thank the Ministry of Education, Culture, Sports, Science, and Technology **(MEXT)** for the financial support through the scholarship program for research students.

Nomenclature

DT	delivery tank (-)
ED	entropy difference (-)
g	gravitational acceleration (m s^{-2})
h	specific enthalpy (kJ kg^{-1})
H_d	delivery head (m)
m	mass (kg)
ORC	Organic Rankine cycle
P	pressure (kPa)
Q	heat (kJ)
R	ideal gas constant for air (kJ kg^{-1} K^{-1})
s	specific entropy (kJ kg^{-1} K^{-1})
T0	ambient temperature (°C)
TDC	top dead center
TP-1	thermal pump type-1
PS-1,2	piston cylinder device-1,2
TP-1B	thermal pump type-1 with incompressible secondary working fluid assumption
TPP	thermal power pump cycle
u	specific internal energy (kJ kg^{-1})
V	volume (m^3)
Va	air tank volume (m^3)
Vp	vapor tank volume (m^3)
VR	volume ratio (-)
Vw	water tank volume (m^3)
W	work done (kJ)
WF	working fluid

Greek symbols

η	efficiency (–)
v	specific volume (m^3 kg^{-1})
ρ	density of water (kg m^{-3})

Subscripts

1-5	thermodynamic states of working fluid
a	air
atm	atmosphere
d	delivery
p	vapor
wf	working fluid

References

1) A. Pal, K. Uddin, K. Thu, and B.B. Saha, “Environmental assessment and characteristics of next generation refrigerants,” *Evergreen*, **5** (*2*) 58–66 (2018). doi:10.5109/1936218.
2) S.M. Ali, and A. Chakraborty, “Performance study of adsorption cooling cycle for automotive air-conditioning,” *Evergreen*, **2** (*1*) 12–22 (2015). doi:10.5109/1500423.
3) F. Jerai, T. Miyazaki, B.B. Saha, and S. Koyama, “Overview of adsorption cooling system based on activated carbon - alcohol pair,” *Evergreen*, **2** (*1*) 30–

40 (2015). doi:10.5109/1500425.
4) I. Yaningsih, M.H. Mahmood, A.T. Wijayanta, T. Miyazaki, and S. Koyama, "Experimental study on dehumidification technology using honeycomb desiccant block," *Evergreen*, **5** (*2*) 11–18 (2018). doi:10.5109/1936212.
5) K.G. Cassman, and P. Grassini, "Can there be a green revolution in sub-saharan africa without large expansion of irrigated crop production?," *Glob. Food Sec.*, **2** (*3*) 203–209 (2013). doi:10.1016/j.gfs.2013.08.004.
6) R.E. Namara, G. Gebregziabher, M. Giordano, and C. De Fraiture, "Small pumps and poor farmers in sub-saharan africa: an assessment of current extent of use and poverty outreach," *Water Int.*, **38** (*6*) 827–839 (2013). doi:10.1080/02508060.2014.847777.
7) A. latha K. V., M. Gopinath, and A.R.S. Bhat, "Impact of climate change on rainfed agriculture in india: a case study of dharwad," *Int. J. Environ. Sci. Dev.*, **3**(*4*) 368–371 (2012). doi:10.7763/ijesd.2012.v3.249.
8) K. Marzia, M.F. Hasan, T. Miyazaki, B.B. Saha, and S. Koyama, "Key factors of solar energy progress in bangladesh until 2017," *Evergreen*, **5** (*2*) 78–85 (2018). doi:10.5109/1936220.
9) S.M. Wazed, B.R. Hughes, D.O. Connor, and J.K. Calautit, "A review of sustainable solar irrigation systems for sub-saharan africa," *Renew. Sustain. Energy Rev.*, **81** (*June 2017*) 1206–1225 (2018). doi:10.1016/j.rser.2017.08.039.
10) R.R. Mankbadi, and S.S. Ayad, "Small-scale solar pumping: the technology," *Energy Convers. Manag.*, **28** (*2*) 171–184 (1988). doi:10.1016/0196-8904(88)90043-X.
11) W. Wong, Y, and K. Sumathy, "Solar thermal water pumping systems: a review," *Renew. Sustain. Energy Rev.*, **3** (*2–3*) 185–217 (1999). doi:10.1016/S1364-0321(98)00018-5.
12) A.M. Delgado-Torres, "Solar thermal heat engines for water pumping: an update," *Renew. Sustain. Energy Rev.*, **13** (*2*) 462–472 (2009). doi:10.1016/j.rser.2007.11.004.
13) D.J. Picken, K.D.R. Seare, and F. Goto, "Design and development of a water piston solar powered steam pump," *Sol. Energy*, **61** (*3*) 219–224 (1997). doi:10.1016/S0038-092X(97)00050-9.
14) R. Burton, "A solar powered diaphragm pump," *Sol. Energy*, **31** (*5*) 523–525 (1983).
15) E. Orda, and K. Mahkamov, "Development of 'low-tech' solar thermal water pumps for use in developing countries," *J. Sol. Energy Eng. Trans. ASME*, **126** (*2*) 768–773 (2004). doi:10.1115/1.1668015.
16) K. Sumathy, "Experimental studies on a solar thermal water pump," *Appl. Therm. Eng.*, **19** (*5*) 449–459 (1999). doi:10.1016/S1359-4311(98)00071-4.
17) J. Sitranon, C. Lertsatitthanakorn, P. Namprakai, N. Prathinthong, T. Suparos, and N. Roonprasang, "Parametric consideration of a thermal water pump and application for agriculture," *J. Sol. Energy Eng.*, **137** (*3*) 031006 (2015). doi:10.1115/1.4029108.
18) H. Jokar, and A.R. Tavakolpour-Saleh, "A novel solar-powered active low temperature differential stirling pump," *Renew. Energy*, **81** 319–337 (2015). doi:10.1016/j.renene.2015.03.041.
19) J. Nihill, A. Date, J. Velardo, and S. Jadkar, "Experimental investigation of the thermal power pump cycle – proof of concept," *Appl. Therm. Eng.*, **134** (*August 2017*) 182–193 (2018). doi:10.1016/j.applthermaleng.2018.01.106.
20) D.P. Rao, and K.S. Rao, "Solar water pump for lift irrigation," *Sol. Energy*, **18** (*5*) 405–411 (1976). doi:10.1016/0038-092X(76)90006-2.
21) K. Sudhakar, M.M. Krishna, D.P. Rao, and R.S. Soin, "Analysis and simulation of a solar water pump for lift irrigation," *Sol. Energy*, **24** (*1*) 71–82 (1980). doi:10.1016/0038-092X(80)90022-5.
22) K. Sumathy, A. Venkatesh, and V. Sriramulu, "Thermodynamic analysis of a solar thermal water pump," *Sol. Energy*, **57** (*2*) 155–161 (1996). doi:10.1016/S0038-092X(96)00050-3
23) R. Bandaru, and C. Muraleedharan, "Performance prediction of solar thermal water pump using artificial neural networks," **15** (*1*) 1–8 (2017). doi:10.5383/ijtee.15.01.001.
24) W. Wong, Y, and K. Sumathy, "Thermodynamic analysis and optimization of a solar thermal water pump," *Appl. Therm. Eng.*, **21** (*5*) 613–627 (2001). doi:10.1016/S1359-4311(00)00065-X.
25) A. Date, and A. Akbarzadeh, "Theoretical study of a new thermodynamic power cycle for thermal water pumping application and its prospects when coupled to a solar pond," *Appl. Therm. Eng.*, **58** (*1–2*) 511–521 (2013). doi:10.1016/j.applthermaleng.2013.05.004.
26) N. Kurhe, A. Funde, P. Gokhale, S. Jadkar, S. Ghaisas, and A. Date, "Development of low temperature heat engine for water pumping application," *Energy Procedia*, **110** (*December 2016*) 292–297 (2017). doi:10.1016/j.egypro.2017.03.142.
27) W. Wong, Y, "Performance of a solar water pump with ethyl ether as working fluid," *Renew. Energy*, **22** (*1–3*) 389–394 (2001). doi:10.1016/S0960-1481(00)00065-3.
28) W. Wong, Y, and K. Sumathy, "Performance of a solar water pump with n-pentane and ethyl ether as working fluids," *Energy Convers. Manag.*, **41** 915–927 (2000). doi:10.1016/S0960-1481(00)00065-3.
29) R. Bandaru, C. Muraleedharan, and P.K. Pavan, "Modelling and dynamic simulation of solar-thermal energy conversion in an unconventional solar thermal water pump," *Renew. Energy*, **134** 292–305 (2019). doi:10.1016/j.renene.2018.10.108.
30) "Klein, s.a.,engineering equation solver (ees), academic commercial v10.644, f-chart software," (n.d.).